Published in final edited form as:
Ultrasound Med Biol. 2013 March ; 39(3): 424–438. doi:10.1016/j.ultrasmedbio.2012.10.012.

HISTOLOGICAL AND BIOCHEMICAL ANALYSIS OF MECHANICAL AND THERMAL BIOEFFECTS IN BOILING HISTOTRIPSY LESIONS INDUCED BY HIGH INTENSITY FOCUSED ULTRASOUND

Yak-Nam Wang,
Center for Industrial and Medical Ultrasound, Applied Physics Laboratory, University of Washington, 1013 NE 40th Street, Seattle WA 98105

Tatiana Khokhlova,
tdk7@u.washington.edu, Tel: +1 206 543 61 93, Fax: +1 206 543 67 85, Division of Gastroenterology, Department of Medicine, University of Washington, 1959 NE Pacific Street, Seattle, WA, 98195 and Center for Industrial and Medical Ultrasound, Applied Physics Laboratory, University of Washington, 1013 NE 40th Street, Seattle WA 98105

Michael Bailey,
Center for Industrial and Medical Ultrasound, Applied Physics Laboratory, University of Washington, 1013 NE 40th Street, Seattle WA 98105

Joo Ha Hwang, and
Division of Gastroenterology, Department of Medicine, University of Washington, 1959 NE Pacific Street, Seattle, WA, 98195 and Center for Industrial and Medical Ultrasound, Applied Physics Laboratory, University of Washington, 1013 NE 40th Street, Seattle WA 98105

Vera Khokhlova
Department of Acoustics, Physics Faculty, Moscow State University, Leninskie Gory, Moscow 119991, Russia and Center for Industrial and Medical Ultrasound, Applied Physics Laboratory, University of Washington, 1013 NE 40th Street, Seattle WA 98105

Abstract

Recent studies have shown that shock wave heating and millisecond boiling in high intensity focused ultrasound (HIFU) fields can result in mechanical fractionation or emulsification of tissue - named boiling histotripsy. Visual observations of the change in color and contents indicated that the degree of thermal damage in the emulsified lesions can be controlled by varying the parameters of the exposure. The goal of this work was to examine thermal and mechanical effects in boiling histotripsy lesions using histological and biochemical analysis. The lesions were induced in *ex vivo* bovine heart and liver using a 2-MHz single-element transducer operating at duty factors of 0.005–0.01, pulse durations of 5–500 ms, and *in situ* shock amplitude of 73 MPa. Mechanical and thermal damage to tissue was evaluated histologically using conventional staining techniques (H&E and NADH-diphorase). Thermal effects were quantified by measuring denaturation of salt soluble proteins in the treated region. According to histology, the lesions that visually appeared as a liquid, contained no cellular structures larger than a cell nucleus and had a very sharp border of 1–2 cells. Both histology and protein analysis showed that lesions obtained

with short pulses (< 10 ms) did not contain any thermal damage. Increasing the pulse duration resulted in an increase in thermal damage. However, both protein analysis and NADH-diaphorase staining showed less denaturation than visually observed as whitening of tissue. The number of HIFU pulses delivered per exposure did not change the lesion shape or the degree of thermal denaturation, whereas the size of the lesion showed a saturating behaviour thus suggesting optimal exposure duration. This study confirmed that boiling histotripsy offers an effective, predictable way to non-invasively fractionate tissue into subcellular fragments with or without inducing thermal damage.

Keywords

high intensity focused ultrasound; HIFU; histotripsy; histology; boiling; lesion; protein analysis; thermal effects

INTRODUCTION

High Intensity Focused Ultrasound (HIFU) therapy is a noninvasive modality for thermal ablation of diseased tissue, e.g. benign and malignant tumors (Dubinsky et al. 2008). In recent years there has been also a significant interest in using HIFU for performing non-invasive tissue emulsification rather than thermal ablation. This effect, later termed histotripsy, was achieved by exposing soft tissues to microsecond duration pulses of HIFU with extremely high peak negative pressures at very low duty cycle (Parsons et al. 2006). The physical mechanism of histotripsy has been attributed to the activity of the cavitation clouds that form at the HIFU transducer focus and their further interaction with the incident HIFU pulse (Maxwell et al. 2011; Simon et al. 2011). The feasibility and promise of histotripsy have been demonstrated in *in vivo* studies for a number of medical applications that involve either cutting through or emulsifying bulk tissue (Owens et al. 2012; Lake et al. 2008). Histotripsy lesions have been shown to contain liquefied tissue with no discernible cellular structure, with a boundary of only a few microns wide (Winterroth et al. 2011). The histotripsy procedures to produce intracardiac septal defects or liquefaction of the prostate resulted in minimal damage to surrounding tissues and blood vessels and were generally well tolerated (Owens et al. 2012; Lake et al. 2008).

An alternative method was recently proposed where another form of HIFU-induced bubble activity – boiling - was used for controllable and predictable tissue emulsification (Canney et al. 2009). This method, termed boiling histotripsy, utilizes relatively lower peak pressures and much longer pulses as compared to the cavitation cloud histotripsy. The physical mechanism of boiling histotripsy has been attributed to the presence of shock fronts in the acoustic waveform at the focus formed because of nonlinear propagation effects, effective tissue heating caused by absorption at the shocks, and repetitive localized initiation of boiling in tissue in as short as a few milliseconds within each pulse (Canney et al. 2010). The explosion of a millimeter-sized boiling bubble and its further interaction with shocks cause mechanical fractionation of tissue and ultimately its complete emulsification (Simon et al. 2011). If the duration of the HIFU pulse is not much longer than the time to reach boiling at the focus, and the duty cycle is low enough to avoid the accumulation of heat, then the thermal injury to tissue is negligible (Khokhlova et al. 2011a).

The major advantage of this method over the conventional, cavitation-based, histotripsy is that boiling in tissue caused by shock wave heating is by nature less stochastic in its occurrence than cavitation, which makes the method that utilizes boiling more predictable and repeatable. It was demonstrated that the pulsing protocol can be designed and adjusted for different tissues and different clinical situations based on the time to reach boiling

temperature at the HIFU focus (Khokhlova et al 2011b). The latter can be reliably predicted theoretically based on the weak shock theory and detected experimentally (Canney et al. 2009). Furthermore, the requirements to the size, focusing gain, and frequency of the HIFU source were shown to be less restricting, therefore the transducer can potentially be miniaturized and incorporated into transrectal or endoscopic devices (Khokhlova et al 2011a).

To date, the lesions produced by boiling histotripsy in *ex vivo* tissues were only evaluated by gross observation. It was therefore difficult to draw quantitative conclusions on the degree of tissue fractionation and the extent of thermal damage. Thermal effects were considered present if the produced tissue homogenate was whiter than the intact tissue. With increasing the pulse duration or the duty factor the contents of the lesion gradually became whiter, and the consistency gradually changed from liquid to paste and, eventually, to solid and dehydrated, thermally denatured tissue (Khokhlova et al 2011a). For convenience, the lesions were classified into three types, based on their appearance: “liquid” – a void filled with clear liquefied tissue with no signs of thermal damage in terms of changing the color, “paste” – void with blanched edges filled with white paste, and “vacuolated thermal” – solid thermal lesion with vaporized core. The goal of the present work was to use biochemical and histological methods to analyze the contents and structure and to quantify the thermal effect in the different types of lesions produced by boiling histotripsy. Although only one pulsing protocol corresponding to a representative lesion from each of the three types was selected for the study, any “in-between” lesion type could be achieved by tuning the pulsing protocol accordingly (Khokhlova et al 2011a). The boiling histotripsy lesions were also compared against a purely thermal lesion in tissue, referred to as “solid thermal” in the text. These lesions were induced in tissue at low power output without boiling.

The experiments were performed in *ex vivo* bovine cardiac and liver tissues. These tissues are different in composition, structure, and blood content, and therefore represent a broad spectrum of biochemical changes that may occur during a boiling histotripsy treatment.

MATERIALS AND METHODS

Experimental setup

The experimental arrangement was similar to that used in the previous studies (Fig.1a) (Khokhlova et al 2011a). The measurements were performed in an acrylic tank filled with filtered and degassed water at room temperature (20°C). The HIFU source was a home-built, single-element, air-backed, piezoceramic transducer of 44 mm aperture and focal length (f-number = 1), operating at the frequency of 2.158 MHz. The transducer was driven by a function generator (Agilent 33250A, Agilent, Palo Alto, CA) and an RF amplifier (300W, ENI A-300, ENI, Rochester, NY). A timing board (NI 6608, National Instruments, Austin, TX) was used to trigger the function generator for various pulsing protocols and was controlled using a custom Labview program (National Instruments, Austin, TX). The HIFU source was attached to a 3-axis positioning system (Velmex Inc., Bloomfield, NY) to align the focus with the desired position within the exposure sample. The time to reach boiling in tissue at the HIFU focus was measured by recording the onset of fluctuations in the transducer excitation voltage using a 10X high-voltage probe attached to a digital oscilloscope (LT344, Lecroy, Chestnut Ridge, NY). The fluctuations represent the transduction of variation in the acoustic impedance of the transducer, caused by the ultrasound backscattered from bubbles. Thus, large mm-sized boiling bubbles appearing at the transducer focus caused the largest fluctuations (Khokhlova et al 2011a).

Tissue sample preparation and positioning

Bovine cardiac and liver tissue was obtained from an abattoir on the same day as experiments and stored in a bag of phosphate buffered saline, on ice. This tissue preservation method is similar to that used in the procedure for organ transplantation, and is known to preserve tissue functionality and viability for up to 72 hours (Lam et al. 1989). Tissue was cut into samples to fit a custom-designed tissue holder (8 cm wide by 8 cm tall by 2.7 cm deep) and was degassed for one hour in a desiccant chamber. In the case of the cardiac tissue, the samples were oriented so that the ultrasound was incident perpendicularly to the muscle fibers.

For focus positioning, a removable "pointer" was attached to the HIFU transducer before each exposure. The tip of the pointer, which coincides with the transducer focus, was aligned with the desired transverse position on the sample surface. The pointer was then removed, and the sample moved towards the transducer in the axial direction, to place the focus at the 12 mm depth within the sample. The individual lesions were spaced 1 cm apart in a rectangular grid. To specify the lateral position of each lesion within the sample, four thermal "marker" lesions were induced at the tissue surface facing the transducer as illustrated in Fig.1b. For each marker, the transducer focus was positioned at the tissue surface, 5 mm away in the lateral direction from the lesion intended for investigation, and a high power (15 kW/cm^2 at the focus) continuous exposure of 1–3 s was delivered until a well defined thermally denatured spot appeared at the surface. After the exposures the tissue samples were cut along the marker rows into cuboids containing individual lesions to avoid the loss of the liquefied tissue (Fig.1b).

Determination of in situ HIFU waveforms

The in situ HIFU waveforms used to induce lesions in *ex vivo* cardiac tissue were determined using a nonlinear derating method described in detail in the publications (Canney et al. 2010; Khokhlova et al. 2011a; Bessonova et al. 2010). The waveforms were "derated" from the data of previously performed characterization of the HIFU transducer field in water at different levels of its excitation. Focal waveforms were simulated in water using the KZK numerical model with a boundary condition calibrated versus measurements (Canney et al. 2008). The derating method allowed to account for ultrasound attenuation in tissue, α, on the way to the focus (Canney et al. 2010; Bessonova et al. 2010) and for the difference of the nonlinear parameters in water, β_{water}, and in tissue, β (Khokhlova et al. 2011a). According to the method, that was described in detail and validated in these previous publications, the in situ focal pressure waveform at a depth l in tissue, at a level of HIFU source excitation p_0, is calculated as follows: 1) Take the focal waveform measured in water at lower source excitation level, p'_0:

$$p'_0 = p_0 \cdot \beta_{water}/\beta \cdot exp(-2\alpha l) \quad (1)$$

2) Multiply the resulting waveform by the ratio β/β_{water}. Here β_{water} =3.5, the values for attenuation and the nonlinear parameter, in bovine cardiac tissue were taken from the previous measurements: α = 0.13 Np/cm, β = 4 (Khokhlova et al. 2011a). The derated focal waveforms are shown in Fig. 2 as thin dashed lines. These waveforms were used to estimate heat deposition rate and time to reach boiling temperature of 100°C in tissue.

To validate the simulation data for *in situ* conditions, pressure waveforms were also measured in water behind a 12-mm thick cardiac tissue sample for the two source power levels used in producing lesions in tissue. The thickness of the sample corresponded to the *in situ* depth of the focus in tissue when producing histotripsy lesions. A fiber-optic probe hydrophone (FOPH) of 100 μm diameter and 100 MHz bandwidth (FOPH 2000, RP

Acoustics, Leutenbach, Germany) was positioned at the spatial maximum of the peak positive pressure. The measured waveforms were deconvolved using the FOPH impulse response provided by the manufacturer and are shown as thick solid curves in Fig. 2. The measured waveforms agree very well with the simulated ones for both power outputs. At high power level, when the shock front was present in the waveform, the peak positive pressure and the shock amplitude in the measurements were 16% lower than in simulations (indicated by arrows in Fig.2a) which has been shown to be due to the limited bandwidth of the hydrophone (Canney et al. 2008).

The highly nonlinear waveform containing a shock front shown in Fig.2a was used to produce different types of boiling histotripsy lesions: liquid, paste, and vacuolated thermal. The shock amplitude, peak positive and peak negative pressures of the numerically calculated and derated waveform were 73 MPa, 67.5 MPa, and 12 MPa, respectively. The corresponding peak *in situ* intensity was calculated by summing the intensities of all harmonics of the fundamental frequency, generated through nonlinear propagation, and was 20 kW/cm^2. The lower amplitude waveform (Fig.2b) was used to create a purely thermal - "solid thermal" - lesion without mechanical effects. The *in situ* peak positive and peak negative pressures were 7.7 MPa and 4.5 MPa, respectively, the peak intensity was 1.7 kW/cm^2.

The *in situ* pressure levels in bovine liver samples were assumed to be approximately the same as in cardiac tissue. The values for attenuation and nonlinearity parameter reported in literature for these tissues are similar (Duck 1990). Moreover, according to the measurements performed in the current study, the measured time to reach boiling at the HIFU focus for both tissues was the same, within the experimental error.

Calculation of time to reach boiling temperature and the choice of exposure parameters

The choice of the exposure parameters, i.e. pulse duration τ and duty factor (*DF*), was based on the time to reach boiling temperature at the focus of the HIFU source t_b and therefore on the *in situ* heating rate H. In the case when high amplitude shocks are present at the focus, the heating rate is mainly determined not by the absorption of the fundamental frequency, but by the *in situ* shock amplitude A_s, and can be calculated using weak shock theory (Hamilton and Blackstock 1989):

$$H=\frac{\beta f_0 A_s^3}{6\rho_0^2 c_0^4}, \quad (2)$$

where β is the coefficient of nonlinearity, f_0 is the ultrasound frequency, c_0 is the ambient sound speed, and ρ_0 is the density of the medium. If the heating rate is high enough so that temperatures of 100°C are reached in tens of milliseconds, heat diffusion has a little effect and can be neglected, therefore, the time-to-boil (t_b) can be estimated as (Khokhlova et al. 2011a):

$$t_b=\frac{\Delta T c_v}{H}, \quad (3)$$

where ΔT is the change from the ambient temperature to 100°C, c_v is the heat capacity per unit volume. The following physical constants were used for calculating time-to-boil in the cardiac and liver tissues: ρ_0 = 1044 kg/m^3, c_0 = 1544 m/s, β = 4.0, $c_v = 5.3\times10^6$ J m^{-3}C^{o-1} (Duck 1990).

The calculated time to reach the boiling temperature at the transducer focus in both liver and cardiac tissue was 4.5 ms. In the experiments, the time to reach boiling was recorded for

each lesion according to the start in the transducer voltage fluctuations during the first HIFU pulse, and was 3.5±1 ms for the cardiac muscle (averaged over 31 samples), which is within the experimental error from the predicted value. The time to reach boiling was somewhat shorter than estimated for the liver tissue (averaged over 13 samples) − 2.5±0.6 ms, most probably because the acoustic attenuation and/or nonlinearity parameter in liver were slightly different from the heart.

Note, that in the present study in *ex vivo* tissue, with well controlled exposure conditions, the theoretically estimated and measured time to reach boiling corresponded relatively well. In the cases of more complex tissues (layered or otherwise), or in the *in vivo* situation, the theoretical prediction may not be as accurate, and may only serve as an initial assessment. The time to boiling measured during the first HIFU pulse would then provide feedback to adjust the pulsing protocol.

The pulsing regimes (the pulse durations and *DF*s) used to produce the three different types of boiling-histotripsy lesions – liquid, paste, and vacuolated thermal – were chosen according to the parameter space defined in Khokhlova et al. (2011a) and are listed in Table 1. In all exposures, the total HIFU-on duration per lesion was 500 ms.

The two different regimes listed in Table 1 for the “paste” lesion in cardiac muscle were used for different purposes: (a) histological evaluation, (b) protein analysis. Regime (a) corresponded to the combination of the shortest pulse duration (t) and the lowest duty factor (DF) at which the thermal effects, defined by visual observation as blanching of the emulsified lesion contents, were observed: $DF = 0.01$, $t = 10$ ms = 2.2 t_b. The histological evaluation of these paste lesions in cardiac muscle indicated, however, that no thermal denature occurred. Regime (b) used for protein analysis in cardiac muscle corresponded to longer pulse duration required to produce paste lesions in liver: $DF = 0.01$, $t = 20$ ms = 4.4 t_b.

A purely thermal lesion typical for conventional HIFU ablation - a “solid thermal” lesion - was produced in continuous mode exposure at the focal *in situ* intensity of 1.7 kW/cm^2 for 20 s, as listed in Table 1. The corresponding focal waveform is shown in Fig.1b. During these exposures no fluctuations of the transducer voltage were detected by the high voltage probe indicating that boiling did not occur. This was also confirmed by modeling the temperature field in tissue during the exposure using the KZK numerical model and the heat transfer equation similarly to Khokhlova et al. (2009). According to the results of the simulations, by the end of the exposure the temperature was only slightly lower than 100°C.

Histology

The tissue cuboids, each containing a single lesion of a certain type, were either frozen embedded (4 samples of each lesion type) or fixed in 10% neutral buffered formalin (2 samples of each lesion type) for histological evaluation.

In order to characterize the thermal damage to tissue, the frozen samples were sectioned longitudinally to the lesion, and sequential 8 μm thick slices were collected from the middle of each lesion. One of the sections was stained with hematoxylin and eosin (H&E), which stains cell nuclei blue/purple, while eosin stains cytoplasm, connective tissue, and other extracellular substances pink or red, thus allowing the visualization of tissue structure and its mechanical disruption. The other section was stained for nicotinamide adenine dinucleotide-diaphorase (NADH-d) activity to evaluate the extent of thermal damage. In this enzyme histological stain, tissue that contains active NADH-d (an enzyme produced by mitochondria) is stained blue/purple and is considered viable; whereas thermally-killed

tissue remains unstained. NADH-d stain is routinely used in evaluation of the results of RF ablation (Date et al. 2005).

The fixed samples were kept in 10% neutral buffered formalin for one week, before being paraffin embedded and sectioned longitudinally to the lesion. A 6 μm slice was collected from the middle of each lesion and stained with H&E. Formalin-fixed tissue for H&E staining is the gold standard for visualization of the tissue pathology and provides sharper images with less artifact than frozen sections. In current work this procedure was used to verify the findings from the frozen samples.

Protein analysis

The following method, that will be referred here to as protein analysis, was utilized to quantify the percentage of thermally denatured protein in the lesion content. This method is based on the effect that hydrophilic proteins, when denatured, lose solubility in water and salt solutions. Soluble proteins were extracted from the samples by a series of water and salt extractions and the concentration of protein in the pooled extractions was measured using traditional protein quantification methods. This approach has been employed in food industry for a long time to evaluate the quality of meat and is applicable to water soluble proteins, such as globular and myofibrillar proteins (Zayas 1997). It is important to note, that most fibrous proteins (e.g. collagen) are insoluble, and their denaturation can not be evaluated using this method. However, in liver and cardiac tissue, the majority of the proteins are hydrophillic. This approach is therefore a good representation of general thermal denaturation of proteins in the tissue.

To collect the lesion content without losing any liquefied tissue, the very top of a tissue cuboid containing a lesion was cut off while maintaining the sample in the vertical position. In the cases of paste and liquid lesions a small pipette was used for sample collection. The contents of the solid and vacuolated thermal lesions were collected by cutting small pieces of tissue from the lesion and then mincing finely using two razor blades. The contents were collected from 3–6 samples of each lesion type. All samples were weighed and subjected to a series of water and salt extractions. In between each extration, the sample was centrifuged and the supernatant was removed and pooled for protein analysis. The amount of extracted protein in the supernatant was evaluated by a colorimetric assay (Coomassie Plus Bradford Protein Assay). A standard protein curve was used to determine the concentration in solution. The concentrations were normalized by the wet weight of the sample to give a number of milligram protein per milligram of tissue.

A small part of each tissue sample, in which the lesions were produced, was used as a positive control. The tissue was homogenized mechanically and underwent the same procedure as all other samples. The concentration of denatured protein in each sample is presented as the percent of denatured protein relative to the corresponding control sample. Statistical differences between the lesion types were calculated using a one-way independent ANOVA and Gabriel’s post-Hoc test.

RESULTS

Histology examination of the frozen samples

This section describes the results of the histological analysis of the various types of lesions, obtained using boiling histotripsy in *ex vivo* tissue. The figures presented in the section are typical examples of the observed tissue damage produced using certain HIFU exposure parameters. Similarly to our previous gross observations, the lesion morphology resulting from one exposure protocol was very repeatable (Khokhlova et al. 2011). The range of lesion morphological parameters (size of debris, sharpness of the border, extent of thermal

damage, observed artifacts), given in the analysis of each lesion type, includes all of the lesions of that type, not only the ones that are shown in the figures.

Photographs of each lesion type induced in bovine cardiac muscle are presented side by side with the representative histological sections stained with H&E and NADH (Fig. 3). Homogenized tissue seen in gross photographs as liquid or paste (ai, bi) corresponds to the extensive disruption of cellular structure seen in the H&E histological sections (aii, bii). The corresponding NADH-stained sections (aiii, biii) do not show evidence for thermal denaturation, (the lesion contents stained as intensive as the surrounding tissue) although gross observation of the paste lesion clearly indicates whitening of its content which is usually viewed as an indication of thermal damage. The solid and vacuolated thermal lesions (cii, dii) are not observed very clearly in the H&E stained sections. The lesion area is only slightly more eosinophylic (stained darker pink) than the surrounding intact tissue. This increase in eosinophylic intensity is likely due to tissue dehydration and is thus an indirect indication of the thermal coagulation of tissue. The large voids seen in the gross photograph of the vacuolated lesion are also observed in the histological sections, whereas there is no major structural disruption in the solid thermal lesion. NADH-stained sections of both types of thermal lesions clearly demonstrate the areas of thermal denature as the absence or lack of blue/purple stain (ciii, diii). The boundary of the solid lesion is much more gradual than that of the vacuolated lesion and includes the areas in which the enzymatic activity is still present, but not to the same degree as in the intact tissue.

Magnified view (Fig. 4) of the lesions stained with H&E (i) and NADH (ii) revealed distinct differences for each lesion type. The margins of both liquid and paste lesions, outlined with dashed lines in all figures, are very sharp: the transition zone of partially damaged cells is only 1–2 cells wide, i.e. 15–40 microns. No large cell remnants or intact cell nuclei are present in the liquid lesion contents, whereas the paste lesion contains some areas of un-emulsified tissue fragments in the range of 15–40 microns (outlined by thin solid lines in bii) The cellular structure of tissue at the borders of both vacuolated (c) and solid (d) thermal lesions is almost fully preserved, and the lesion boundaries are hardly noticeable in H&E stained sections. The margin between thermally damaged and intact tissue, according to the NADH-stained sections, is much more gradual in the solid thermal lesion (on the order of 100 microns) than in the vacuolated lesion (on the order of 50 microns). Unlike the margin region, the cellular structure at the core of the vacuolated thermal lesion (green arrows in ei and eii) is substantially disrupted. Tissue fragments, that are still present between the large voids, are shrunken, but still have some semblance of cellular structure. The nuclei (indicated by black arrowheads in ei) show evidence of pyknosis (condensation of chromatin in the nucleus) or subsequent karyorrhexis (fragmentation of the nucleus) as indicated by small and dense darkly stained structures.

Photographs of the gross lesions and the histological sections of lesions induced in bovine liver tissue are compared in Fig. 5. The tissue sections stained with NADH have a slightly different hue, purple rather than blue, compared to the bovine cardiac muscle due to the difference in cellular structure and mitochrondria content and architecture. Similarly to the case of cardiac muscle tissue, the histological sections of the liquid lesion indicate the destruction of cellular structure and the absence of thermal damage. The NADH stain of the paste lesion, however, shows isolated areas of unstained, i.e. thermally-killed, tissue debris within the lesion contents. Frozen tissue artifact – large elongated ice crystals aligned in groups - is very pronounced within the lesion, indicating that the lesion contents is liquefied.

The vacuolated thermal lesion is visible in the H&E-stained histological section as a slightly more eosinophylic region with multiple large voids. The lesion border is more distinct in the NADH-stained section, and has varying shades of stain indicating a gradient of the amount

of acitve enzyme. The tissue immediately adjacent to the large vacuoles has a slight brown tint due to stronger tissue dehydration and shrinking at the most intensely heated areas. The vacuolated core is surrounded by a thin intensely blue ring followed by a broader ring of unstained, i.e. thermally denatured, tissue. Closer examination revealed this dark blue ring to be an extracellular deposition and can not be mistaken for true enzymatic activity (data not shown). This is an artifact of the stain, but its presence does not alter the interpretation of the slides.

The border of the solid thermal lesion is, again, hardly visible on the H&E-stained tissue section: the liver tissue structure is not disrupted, and is only slightly more eosinophylic at the very core of the lesion. The NADH-stained section shows a well-demarcated region of thermal denature, that, similarly to the vacuolated thermal lesion, has several gradations of hue. The brown-tinted core corresponds to the area around the HIFU focus, in which tissue temperature and, therefore, degree of dehydration, was the highest. The artifactual formazan deposition (intensely blue ring) adjacent to the lesion boundary is also present in the solid thermal lesion.

The magnified view of the different lesion types induced in bovine liver also revealed differences in lesion type (Fig. 6). Similarly to the lesions in cardiac tissue, the margins (outlined by dashed lines) of the liquid (a) and paste (b) lesions are only 1–2 cells wide, whereas in cases of the vacuolated (c) and solid (not shown) thermal lesions the transition zone is more gradual. The contents of the paste lesion is mostly homogenized, with some intact nuclei still present (indicated by black arrowheads in bi), but the intact tissue fragments are of a smaller scale compared to the paste lesion in cardiac muscle. Some areas of the homogenate appear thermally-killed (indicated by black arrow in bii). Similarly to cardiac muscle, cellular structure at the core of the vacuolated thermal lesion (d) is completely disrupted and fully thermally-killed. At the center of the solid thermal lesion (e) the general liver structure was preserved, with the cords of hepatocytes still intact (black ovals), but also fully thermally-killed.

Histology examination of the formalin-fixed samples

H&E-stained sections of formalin-fixed tissue provide a clearer representation of tissue structure compared to fresh-frozen tissue, but they can not be used for viability staining. In the present study the formalin-fixed samples were used to obtain a better estimate of the size and structure of tissue debris present in the liquid and paste lesions and to verify the sharpness of the lesion margins with regards to tissue disruption.

Magnified images (Fig. 7) of the H&E-stained sections of fresh-fozen (i) and formalin-fixed (ii) liquid (a) and paste (b) lesions in cardiac muscle (I) and liver (II) tissue demonstrate the differences between fixed and unfixed tissue. The images of the paste and liquid lesion contents in the fresh-frozen sections are distorted by freezing artifact – the formation of ice crystals in liquids, which in turn results in appearance of columnar shaped voids. This artifact is especially pronounced in the fresh-frozen section of paste lesion in liver (II ai). This makes it difficult to estimate the size of tissue remnants within the homogenate. The formalin-fixed sections provide very clear images of the tissue debris of up to 80 microns in size and several intact nuclei within the paste lesions. No discernible tissue remnants are seen within the liquid lesion in either tissue. Images of formalin-fixed tissue also confirm the sharpness of the liquid and paste lesion margins: the transition zone is only 10–20 microns.

Protein analysis

Figure 8 shows the results of the protein analysis of the four lesion types – liquid, paste, solid thermal, and vacuolated thermal – induced in bovine cardiac muscle (a) or liver (b)

tissue. The liquid lesions in both tissues were found not to contain substantial denatured protein, which is in accord with gross and histological observations. The soluble protein content in the paste lesions was only partly denatured: 22% in case of cardiac muscle and 27% in case of liver tissue. Therefore, the white appearance of the paste contained in the boiling histotripsy lesion does not imply its full thermal coagulation. The degree of denaturation of solid and vacuolated thermal lesions is different for the two tissues. In liver, the tissue within both lesion types was found to be 90% denatured, whereas the viability staining of these lesions indicated full thermal necrosis. In the cardiac muscle the percentage of denatured salt soluble protein was 70% and 75% for the solid and vacuolated thermal lesions, respectively, which is even lower than the corresponding values obtained for the liver tissue.

Dependence of the lesion size and contents on the number of HIFU pulses

The dependencies of the lesion size and contents on various boiling histotripsy exposure parameters – *in situ* HIFU pressure and shock amplitude, pulse duration, duty factor and frequency – have been investigated previously (Khokhlova et al. 2011a and Canney et al. 2009). However, to date it was not clear, how the size, shape and contents of the lesion evolve over the course of the treatment, i.e. with the number of HIFU pulses delivered. Figure 9 shows a series of paste lesions induced in cardiac muscle tissue using the increasing number of HIFU pulses and the pulsing protocol (a) from the Table 1. First, note that the contents of the lesion (paste) did not change with the number of pulses, which indicates that the degree of thermal denature did not depend on the total HIFU energy delivered using this protocol with low duty factor. The length, L, and maximum width, W, of the lesion changed gradually with the number of pulses until it reached 30 (W=1.8 mm, L=6.3 mm), and then saturated: the dimensions of the lesions produced by 60 (W=2.2 mm, L=6.4 mm) and 90 (W=2.3 mm, L=6.4 mm) pulses are practically the same. This observation appeared to be independent of the lesion type (paste or liquid) and was the same for both tissue types (data not shown).

A lesion produced by a single HIFU pulse alongside with a lesion produced by 30 pulses is shown in Fig.9, in the inset on the right. The single-pulse lesion contains a very narrow, blanched region corresponding to the super-localized focal area of the nonlinear HIFU beam that is heated by shocks to high temperature (Canney et al. 2010). This part of the lesion is thermally denatured and is likely to be formed before the formation of the boiling bubble. A small circular dimple with slightly blanched edges is located in front of the lesion and most probably results from the first explosion of the boiling bubble and its interaction with incident shock waves and is a precursor of the formation of the general tadpole shape of the lesion by subsequent pulses.

DISCUSSION AND CONCLUSIONS

In this work the lesions induced using the boiling histotripsy approach in *ex vivo* bovine cardiac and liver tissues were investigated by histological and biochemical methods. Lesions with varying degrees of thermal damage, referred to as “liquid”, “paste”, and “vacuolated thermal” – were produced by increasing the HIFU pulse duration and the duty factor.

Although lesions of all types were created using a boiling bubble produced in several milliseconds during each pulse and its interaction with the shocks, the lesion contents, at the micoscopic level, were different. Histological evaluation of the liquid lesion in both tissue types revealed that the lesion contained tissue homogenate with no apparent cellular structure or intact nuclei present. In paste lesions, larger cell fragments and some intact nuclei were observed. The core of the vacuolated thermal lesion contained areas of

disrupted, shrunken tissue that still maintained some cell structure, whereas the boundary appeared thermally fixed, with little mechanical disruption.

An explanation for these differences is offered by the mechanism of tissue fractionation that was recently hypothesized - the formation of a miniature acoustic fountain into the boiling bubble or ultrasound atomization of tissue (Simon et al. 2011). The millimeter-sized boiling bubble that forms at the HIFU focus can be considered as a tissue-vapor interface, at which the shock waves are incident for the rest of each HIFU pulse. A narrow area of tissue border, corresponding to the focal beam width, is then pushed into the boiling bubble by acoustic radiation force, thus creating a tissue “fountain” into the bubble. Formation of the fountain is accompanied by atomization of tissue or tearing of small tissue fragments off the tissue-vapor interface. Similarly to the atomization of liquids, multiple mechanisms may be involved in the this process (Rozenberg 1973). Instabilities in capillary waves formed at the interface of the fountain in liquids cause the separation of micro-droplets, however, this mechanism is unlikely to occur in tissue due to the presence of cell structure. Thin layers of tissue may be torn off due to the extremely high rarefactional pressure generated as the shock fronts are reflected from the free boundary of the boiling bubble. Interference of the shock waves reflected from the bubble with the incident shock-waves was shown to result in a standing wave with extremely high peak negative pressure, which in turn leads to formation of a cavitation bubble cloud (Maxwell et al. 2011). This may further weaken the cellular structure adjacent to the bubble.

According to the hypothesized mechanism, if the incident HIFU pulse is not much longer than the time to reach boiling, the tissue immediately adjacent to the boiling bubble becomes atomized, but not thermally denatured. However, as the duration of HIFU pulse increases, i.e. shock waves continue to arrive and heat tissue, a layer of denatured tissue forms in front of the bubble, and is then atomized. Once globular proteins in tissue become denatured, they form insoluble protein aggregates that contribute to an increase in tissue stiffness (Bharat et al. 2005; Raccosta et al. 2010; Phlhammer and O’Brien 1981) and this might explain the presence of larger cellular fragments and nuclei in the paste lesion. According to the NADH-d stain, these fragments indeed appear as thermally killed in liver tissue, but this was not as apparent in cardiac tissue. This may be due to the inherent variations in NADH-d staining that exists between liver and cardiac tissue. Unlike hepatocytes, myocytes have inhomogeneous enzymatic activity corresponding to focal arrangements of the myofibrills resulting in subtle changes in colour intensity of the formazan possibly being difficult to detect. In the case of the vacuolated thermal lesion, the incident pulse is so long that, later in the pulse, a layer of thermally coagulated tissue around the boiling bubbles inside the lesion becomes too stiff to be atomized. After HIFU is turned off, boiling bubbles shrink and leave large voids. The thermally killed, shrunken and deformed tissue seen between the voids in the histological images probably represent the tissue layers between the boiling bubbles. The presence of a small amount of cell debris in these lesions could have been deposited by the initial atomization process before being thermally denatured.

Three different techniques were used in the current study to evaluate thermal damage to tissue within and around the lesions: gross visual observation based on tissue blanching, histology based on the NADH-d stain, and protein analysis of the lesion contents. The results of visual observation generally corresponded well to the histological findings in both liver and cardiac tissue. A notable exception was found for paste lesion in cardiac tissue, in which the content looked blanched visually, but appeared not to be thermally killed histologically.

This effect was observed in paste-type lesions at the shortest duration of the HIFU pulses, when blanching of the lesion content occurred. This may be partially due to inhomogeneous

enzymatic activity found in muscle tissue. It is also proposed that this blanching of tissue without thermal coagulation is better explained by the source of the pigment change after heating. The heme iron, attached to myoglobin and hemoglobin, is responsible for the red pigment in fresh tissue. When heated, oxidation of the heme component results in a pigment change from red to light tan due to the formation of a hemichrome pigment. It is likely that oxidation of the heme iron can occur at a lower temperature than is required for thermal coagulation of cells. This would result in a tan apearance in the tissue before thermal coagulation and enzyme deactivation occur, as indicated by the NADH-d stain.

An artifact of NADH-d stain was observed in thermal lesions in liver tissue - a thin, intensely blue/black ring, that was present close to the edge of the thermally killed tissue (unstained area). This is an artifact that stems from high lipid content of the liver. The formazan formed during the staining process has a high affinity for lipid and can result in secondary, but false positive staining. This ring observed is likely due to lipid, that is liquefied and pushed out of the central heated focal area region, resulting in a blue/black extracellular precipitate (Novikoff et al. 1961).

A small lesion resulting from a single 10-millisecond pulse (inset in Fig.9) was found in the cardiac tissue. The shape of the lesion was symmetric and size corresponded to the superfocused narrow region of heating from the shock waves (Canney et al. 2010; Canney et al. 2008). This observation suggests initial thermal damage of tissue in a very small volume before mm-sized boiling bubble forms and results in mechanical damage of tissue in much bigger volume (Fig. 9). This result is also in accord with the thermal dose *(TD)* formulation that is used to estimate the threshold for tissue thermal necrosis:

$$TD(t)=\int_0^t R^{43-T(t')}dt' \quad (4)$$

where t is treatment time, and $R = 0.25$ if $T(t) < 43°C$ and 0.5 otherwise (Sapareto and Dewey 1984). According to Sapareto and Dewey (1984), the thermal dose required to create a thermal lesion is 240 equivalent minutes. In the present case, as discussed above, the small elongated thermal lesion around the focus was most probably formed before boiling was initiated, i.e. in approximately 4 ms. For this short exposure time the heat diffusion has been shown to be insignificant even in the case of the superlocalized shock wave heating (Canney et al. 2010). The tissue temperature thus can be assumed to increase linearly from 20°C to 100°C in 4 ms. Following this assumption in the Eq. (4), the threshold for thermal denature is reached at 1.2 ms in the center of the lesion, and at 4 ms the *TD* exceeds the threshold by several orders of magnitude. Therefore, although the concept of TD was initially introduced for slow hyperthermia treatments, it likely to be applicable to the present case of rapid, millisecond heating.

In accord with the histological findings, the results of protein analysis indicated that soluble proteins are fully intact within the liquid lesions. In the paste lesions, only 20–30% of protein is denatured, albeit their blanched appearance. However, the vacuolated thermal and solid thermal lesions, that appeared completely denatured both histologically and visually, were shown to contain up to 30% of un-denatured protein. This is most probably an artifact arising from the fact that collagen becomes soluble when denatured to gelatin. With heating of the tissue, all soluble proteins would denature and aggregate becoming insoluble, but insoluble collagen would become soluble. This is one limitation of this protein analysis method used to calculate denatured proteins as it does not account for this opposite process in solubility of the collagen and results in the percent of denatured proteins being less than 100%. This would also explain the difference in denatured protein between liver and cardiac

tissue for both the vacuolated thermal and solid thermal lesions. Cardiac tissue contains significanly more insoluble collagen compared to liver tissue and, when denatured, it will contain a higher amount of soluble protein compared with liver tissue. This will lead to a smaller calculated amount of denatured protein for the cardiac tissue as observed in these studies. However, this solubility assay is a well established method for evaluating protein denaturation in the food industry, and is a good representation of general protein denaturation given the majority of liver and heart proteins are considered soluble. Future studies will include a thorough evaluation of the individual protein components (globular, myofibrillar, and stromal proteins).

Histological images presented here demonstrated the ability of boiling histotripsy to produce highly localized and sharply demarcated mechanical damage to tissue only within the targeted region, leaving the surrounding tissue unaffected. The width of the margins of HIFU-induced thermal lesions is usually reported to be of 5–10 cell lengths or 100–200 microns (ter Haar et al. 1995; Wu et al. 2006; Parmentier et al. 2009; Klingler et al. 2008). The findings of the present study agrees very well with these values: according to NADH-d-stained sections, the boundary of thermal lesions also ranged within 100–200 microns. However, the margins of the emulsified lesions were found to be demarcated with even better sharpness: the transition between completely homogenized and fully intact and viable tissue did not exceed 1–2 cell lengths or 15–40 micron, which agrees very well with the histological findings in cavitation-based histotripsy lesions (Winterroth et al. 2011).

Tissue fractionation was shown to be confined to the focal region, where nonlinear propagation effects are strong, shock waves and enhanced heating are present, and boiling occurs within milliseconds. As nonlinear effects are almost negligible beyond the focal region, collateral mechanical or thermal damage to the surrounding tissues will be relatively suppressed for boiling histotripsy. In this respect, boiling histotripsy technique can be beneficial for certain applications to conventional HIFU-induced thermal ablation, that was shown to sometimes produce thermal damage outside of the targeted area, especially to reflective pre-focal structures such as ribs (Miller et al. 2012; Jung etal. 2011). Recent studies on cavitation-based histotripsy and boiling-based histotripsy have shown the potential to utilize these nonlinear HIFU exposures to effectively irradiate through ribs (Kim et al. 2011; Khokhlova et al. 2011c).

It is interesting to compare the evolution of a liquid lesion shape over the course of boiling histotripsy exposures with the process of cavitation cloud histotripsy. The latter technique is known to produce small liquefied voids scattered throughout the focal region, that enlarge over the course of the treatment and eventually merge to form a single lesion (Roberts et al. 2006). As shown in this study, in boiling histotripsy, several initial HIFU pulses form a single tadpole-like lesion, that only gets enlarged during subsequent pulses (Fig.9). After a certain number of pulses has been delivered, the lesion size reaches saturation, which means that there is an optimal duration of a single treatment. These findings are consistent with the previous observations of boiling histotripsy exposures in transparent polyacrylamide gel phantoms: the lesion dimensions are determined primarily by the size of the boiling bubble produced during each HIFU pulse (Khokhlova et al. 2011a). The maximum size of the boiling bubble depends on the width of the heated region around the focus. As heat transfer processes reach equilibrium in between the pulses, the bubble size reaches the maximum and does not change, and neither does the lateral size of the lesion. We speculate that the length of the lesion is determined by the axial dimension of the HIFU focal region rather than the heating processes. The growth of the lesion in direction towards the transducer is most probably limited by the presence of shocks with high enough amplitude to cause tissue atomization. Once the lesion edge moves out of the focal region in the axial direction, the atomization stops, and so does the lesion growth. The “tail” of the lesion is most probably

formed by streaming of the liquefied tissue within the forming “head”, and it size also saturates as the “head” stops growing.

The work presented herein offers first histological and bio-chemical confirmation that boiling histotripsy is an efficient tool for mechanical fractionation of tissue into subcellular-sized debris, with predictable degree of thermal damage. However, the outcomes of the boiling histotripsy exposures in *ex vivo* tissue reported here may not result in the same outcomes *in vivo*. Due to the blood flow, once a small void is formed by the first HIFU pulse, it is filled with blood which can alter the influence of the subsequent pulses. Cardiac and respiratory motion may lead to a shift in the HIFU focus location, so that each millisecond pulse will induce boiling at a different site, and the shape of the resulting lesion will be altered. Therefore, although the general proof of feasibility of the technique *in vivo* has been reported (Khokhlova et al. 2011b), a thorough bio-chemical and histological characterization is needed and will be performed in our future work.

Acknowledgments

This work was supported by the National Institute of Health (DK43881, EB0007643 and 1K01EB015745) and NSBRI through NASA NCC 9–58. We thank Julianna C. Simon for assistance in experiments, Oleg A. Sapozhnikov for fruitful discussions and the staff and researchers at the Center for Industrial and Medical Ultrasound (CIMU) for help and advice. We are also grateful to staff at the DERC Cellular and Molecular Imaging Core at the University of Washington for help with processing of fixed tissue samples for histology.

REFERENCES

Bharat S, Techavipoo U, Kiss MZ, Liu W, Varghese T. Monitoring stiffness changes in lesions after radiofrequency ablation at different temperatures and durations of ablation. Ultrasound Med Biol. 2005; 31:415–422. [PubMed: 15749565]

Canney M, Khokhlova V, Bailey M, Sapozhnikov O, Crum L. Acoustic characterization of high intensity focused ultrasound fields: A combined measurement and modeling approach. J Acoust Soc Am. 2008; 124:2406–2420. [PubMed: 19062878]

Canney M, Khokhlova V, Bessonova O, Bailey M, Crum L. Shock-induced heating and millisecond boiling in gels and tissue due to high intensity focused ultrasound. Ultrasound Med Biol. 2010; 36:250–267. [PubMed: 20018433]

Canney, M.; Khokhlova, V.; Hwang, JH.; Khokhlova, T.; Bailey, M.; Crum, L. Tissue erosion using shock wave heating and millisecond boiling in high intensity ultrasound field; Proc. 9th International Symposium on Therapeutic Ultrasound; 2009. p. 36-39.

Date RS, Biggins J, Paterson I, Denton J, McMahon RF, Siriwardena AK. Development and validation of an experimental model for the assessment of radiofrequency ablation of pancreatic parenchyma. Pancreas. 2005; 30:266–271. [PubMed: 15782106]

Dubinsky TJ, Cuevas C, Dighe MK, Kolokythas O, Hwang JH. High-intensity focused ultrasound: current potential and oncologic applications. AJR Am J Roentgenol. 2008; 190:191–199. [PubMed: 18094311]

Duck, F. Physical properties of tissue: a comprehensive reference book. London: Academic Press Limited; 1990. p. 9-137.

Hamilton, M.; Blackstock, D. Nonlinear Acoustics. London: Academic Press; 1998. p. 284

Jung SE, Cho SH, Jang JH, Han JY. High-intensity focused ultrasound ablation in hepatic and pancreatic cancer: complications. Abdom Imaging. 2011; 36:185–195. [PubMed: 20512487]

Khokhlova T, Canney M, Lee D, Marro K, Crum L, Khokhlova V, Bailey M. Magnetic resonance imaging of boiling induced by high intensity focused ultrasound. J Acoust Soc Am. 2009; 125:2420–2431. [PubMed: 19354416]

Khokhlova TD, Canney MS, Khokhlova VA, Sapozhnikov OA, Crum LA, Bailey MR. Controlled tissue emulsification produced by high intensity focused ultrasound shock waves and millisecond boiling. J Acoust Soc Am. 2011a; 130:3498–3510. [PubMed: 22088025]

Khokhlova TD, Simon JC, Wang YN, Paun M, Starr FL, Khokhlova VA, Crum LA, Hwang JH, Kaczkowski PJ, Bailey MR. *In vivo* tissue emulsification using millisecond boiling induced by high intensity focused ultrasound. J Acoust Soc Am. 2011b; 129:2477.

Khokhlova, VA.; Yuldashev, PV.; Bobkova, SM.; Ilyin, SA. The role of nonlinear propagation effects in ablation of soft tissue behind the rib cage using a HIFU phased array. 11th Int. Symp. on Therapeutic Ultrasound; New York. 2011 Apr. p. 52

Kim Y, Wang T-Y, Zhen Xu, Cain CA. Lesion generation through ribs using histotripsy therapy without aberration correction. IEEE Trans. Ultrason. Ferroelectr. Freq. Control. 2011; 58(11): 2334–2343. [PubMed: 22083767]

Klingler HC, Susani M, Seip R, Mauermann J, Sanghvi N, Marberger MJ. A Novel approach to energy ablative therapy of small renal tumours: laparoscopic high-intensity focused ultrasound. European Urology. 2008; 53:810–818. [PubMed: 18069120]

Lake AM, Hall TM, Kieran K, Fowlkes JB, Cain CA, Roberts WW. Histotripsy: minimally invasive technology for prostatic tissue ablation in an *in vivo* canine model. Urology. 2008; 72:682–686. [PubMed: 18342918]

Lam FT, Mavor AID, Potts DJ, Giles GR. Improved 72-hour renal preservation with phosphate-buffered sucrose. Transplantation. 1989; 47:767–771. [PubMed: 2655211]

Maxwell AD, Wang T-Y, Cain CA, Fowlkes JB, Sapozhnikov OA, Bailey MR, Xu Z. Cavitation clouds created by shock scattering from bubbles during histotripsy. J Acoust Soc Am. 2011; 130:1888–1898. [PubMed: 21973343]

Miller DL, Smith NB, Bailey MR, Czarnota GJ, Hynynen K, Makin IS. Overview of therapeutic ultrasound applications and safety considerations. J Ultrasound Med. 2012; 31:623–634. [PubMed: 22441920]

Novikoff AB, Shin WY, Drucker J. Mitochondrial localization of oxidative enzymes: staining results with two tetrazolium salts. J Biophys Biochem Cytol. 1961; 9:47–61. [PubMed: 13729759]

Bessonova OV, Khokhlova VA, Canney MS, Bailey MR, Crum LA. A derating method for therapeutic applications of high intensity focused ultrasound. Acoust. Phys. 2010; v 56(No 3):376–385.

Owens GE, Miller RM, Owens ST, Swanson SD, Ives K, Ensing G, Gordon D, Xu Z. Intermediate-term effects of intracardiac communications created noninvasively by therapeutic ultrasound (histotripsy) in a porcine model. Pediatr Cardiol. 2012; 33:83–89. [PubMed: 21910018]

Parmentier H, Melodelima D, N'Djin A, Chesnais S, Chapelon JY, Rivoire M. High-intensity focused ultrasound ablation for the treatment of colorectal liver metastases during an open procedure study on the pig. Ann Surg. 2009; 249:129–136. [PubMed: 19106688]

Parsons J, Cain C, Abrams G, Fowlkes J. Pulsed cavitational ultrasound therapy for controlled tissue homogenization. Ultrasound Med. Biol. 2006; 32:115–129. [PubMed: 16364803]

Pohlhammer J, O'Brien WD Jr. Dependence of the ultrasonic scatter coefficient on collagen concentration in mammalian tissues. J Acoust Soc Am. 1981; 69:283–285. [PubMed: 7217526]

Raccosta S, Manno M, Bulone D, Giacomazza D, Militello V, Martorana V, San Biagio PL. Irreversible gelation of thermally unfolded proteins: structural and mechanical properties of lysozyme aggregates. Eur Biophys J. 2010; 39(6):1007–1017. [PubMed: 19568740]

Roberts WW, Hall TL, Ives K, Wolf JS, Fowlkes JB, Cain CA. Pulsed cavitational ultrasound: a noninvasive technology for controlled tissue ablation (histotripsy) in the rabbit kidney. J Urol. 2006; 175:734–738. [PubMed: 16407041]

Rozenberg, L., editor. Physical principles of ultrasonic technology. Vol. Vol. 2. New York: Plenum Press; 1973. (English – p. 4–88).

Sapareto S, Dewey W. Thermal dose determination in cancer therapy. Int J Radiat Oncol, Biol, Phys. 1984; 10:787–800. [PubMed: 6547421]

Simon J, Sapozhnikov OA, Khokhlova VA, Khokhlova TD, Bailey MR, Crum LA. Miniature acoustic fountain as a possible mechanism for tissue emulsification during millisecond boiling in HIFU fields. J Acoust Soc Am. 2011; 129:2478.

ter Haar G. Ultrasound focal beam surgery. Ultrasound Med Biol. 1995; 21:1089–1100. [PubMed: 8849823]

Winterroth F, Xu Z, Wang T-Y, Wilkinson JE, Fowlkes JB, Roberts WW, Cain CA. Examining and analyzing subcellular morphology of renal tissue treated by histotripsy. Ultrasound Med Biol. 2011; 37:78–86. [PubMed: 21144960]

Wu F, Wang Z-B, Cao Y-D, Xu Z-L, Zhou Q, Zhu H, Chen W-Z. Heat fixation of cancer cells ablated with high-intensity–focused ultrasound in patients with breast cancer. Am J Surg. 2006; 192:179–184. [PubMed: 16860626]

Zayas, JF. Functionality of proteins in food. Berlin: Springer; 1997. p. 6-75.

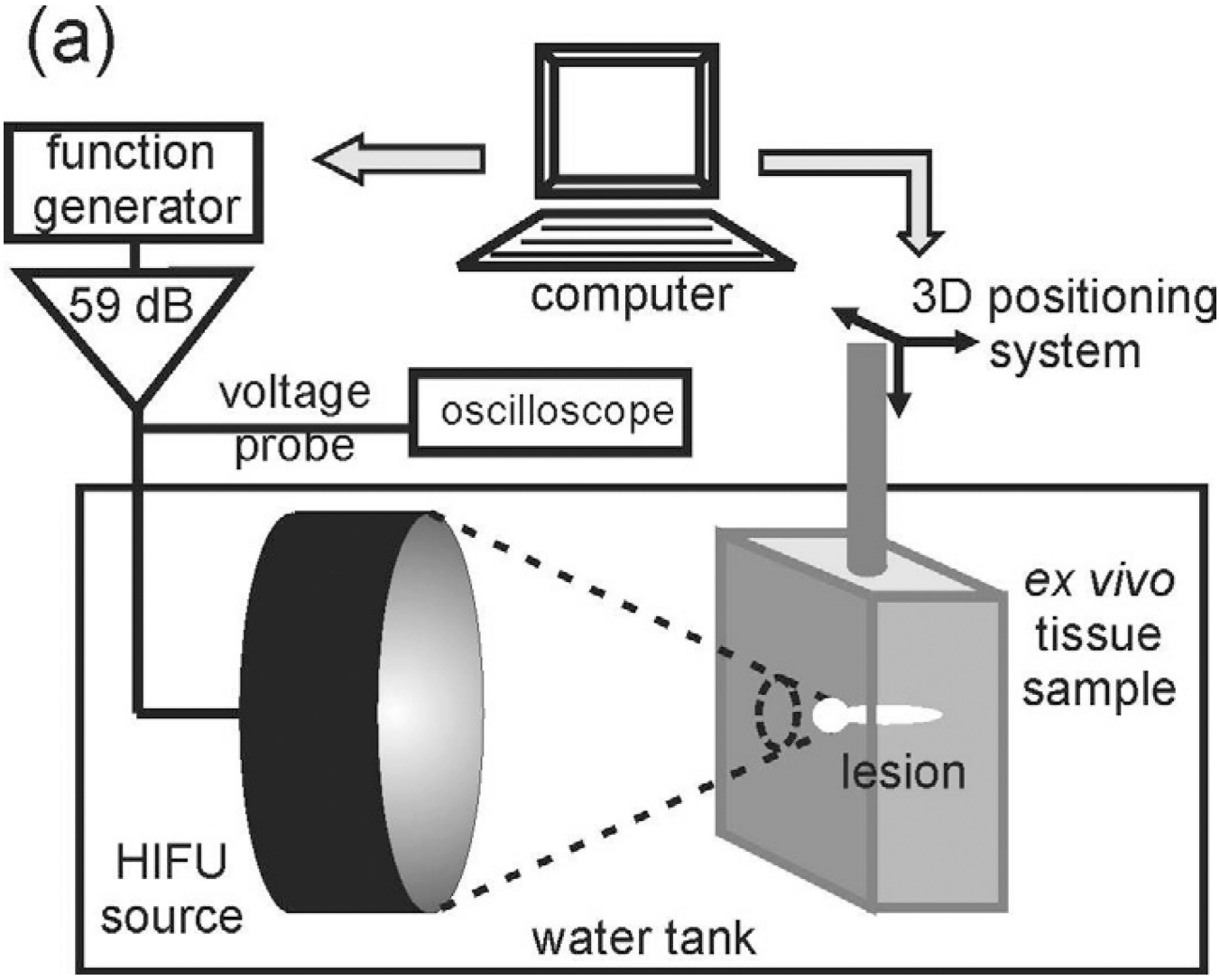

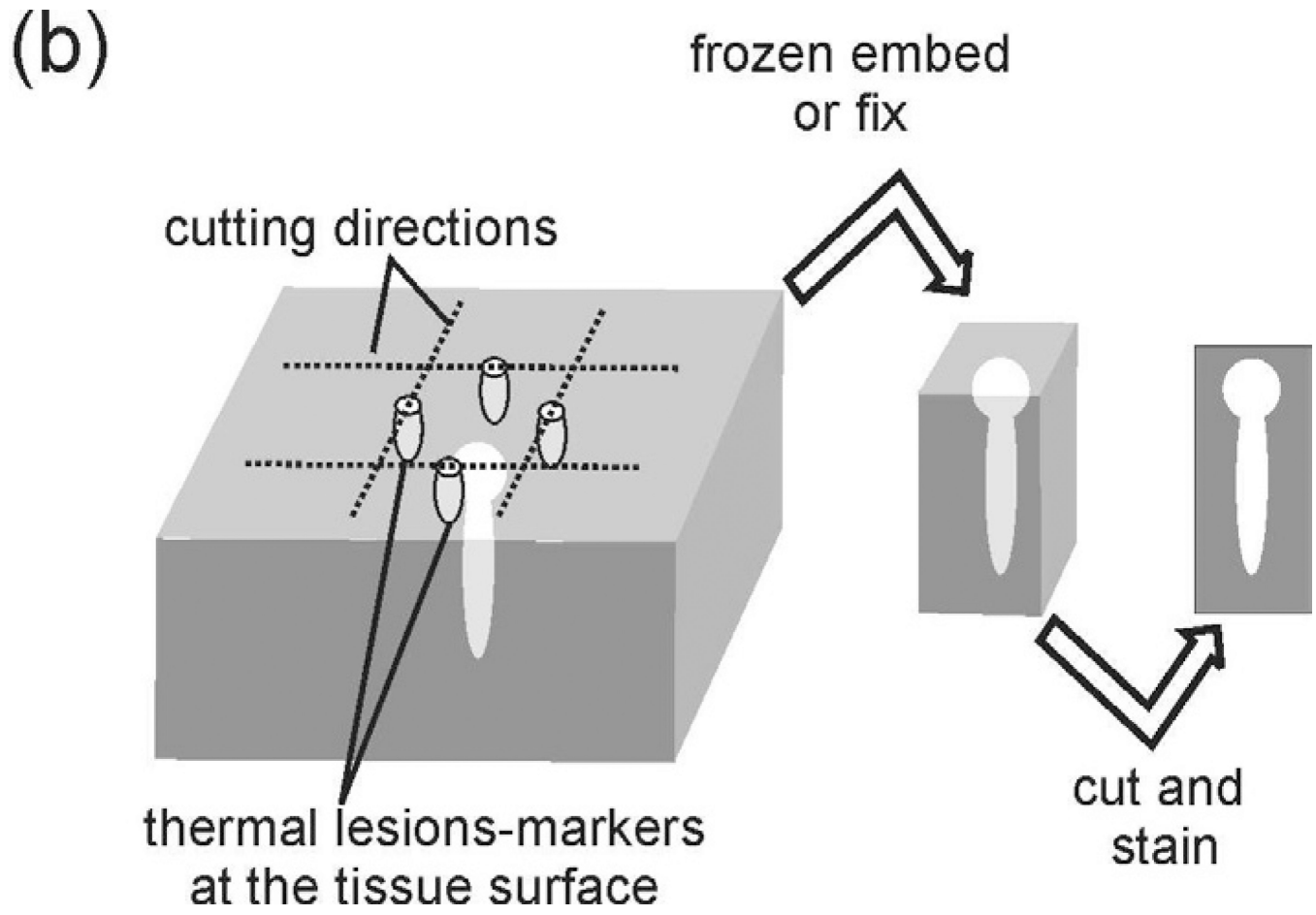

Figure 1.
(a) A diagram of the experimental setup that was used to produce HIFU lesions in *ex vivo* tissue samples. **(b)** Illustration of the protocol of histology samples preparation.

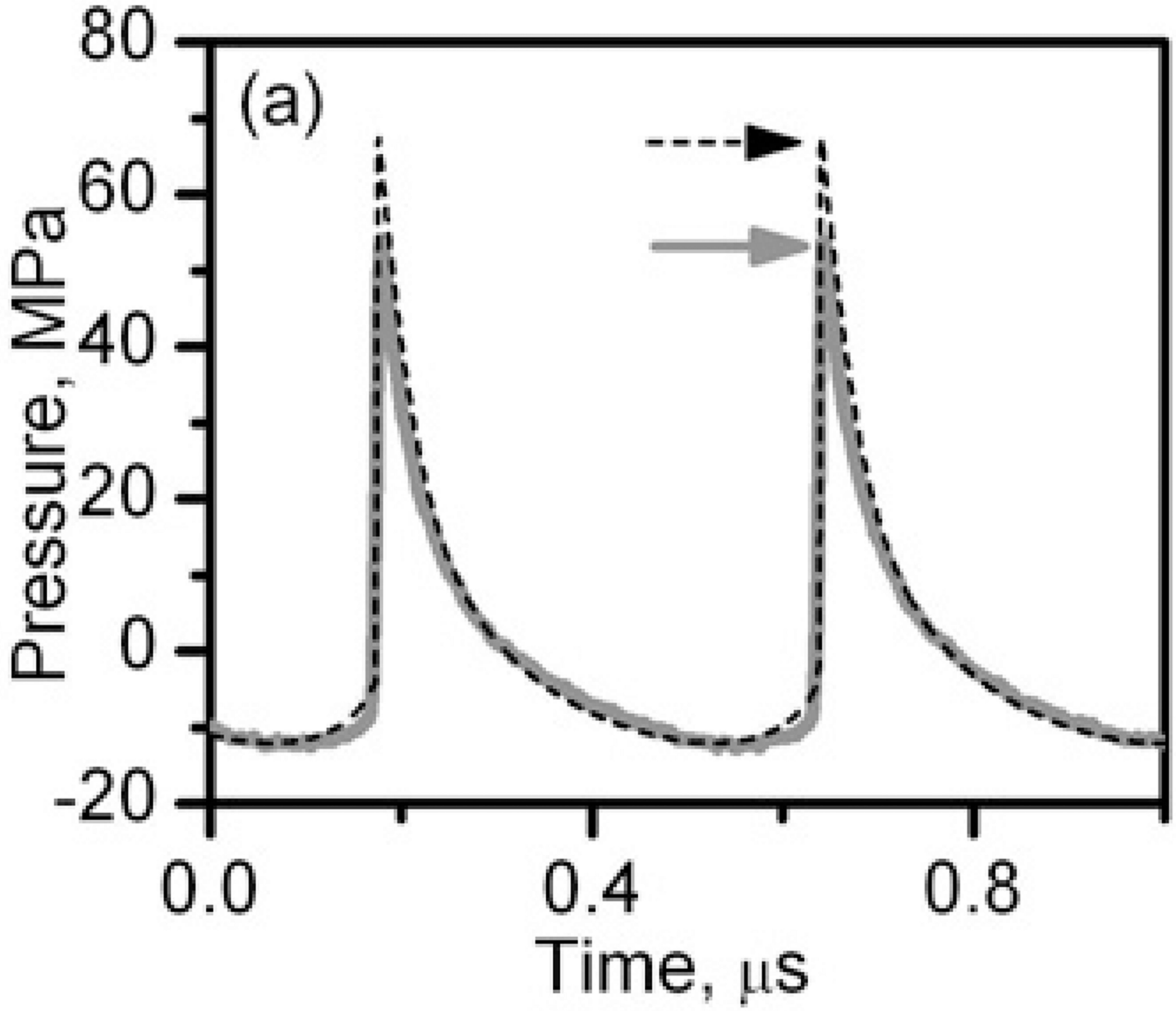

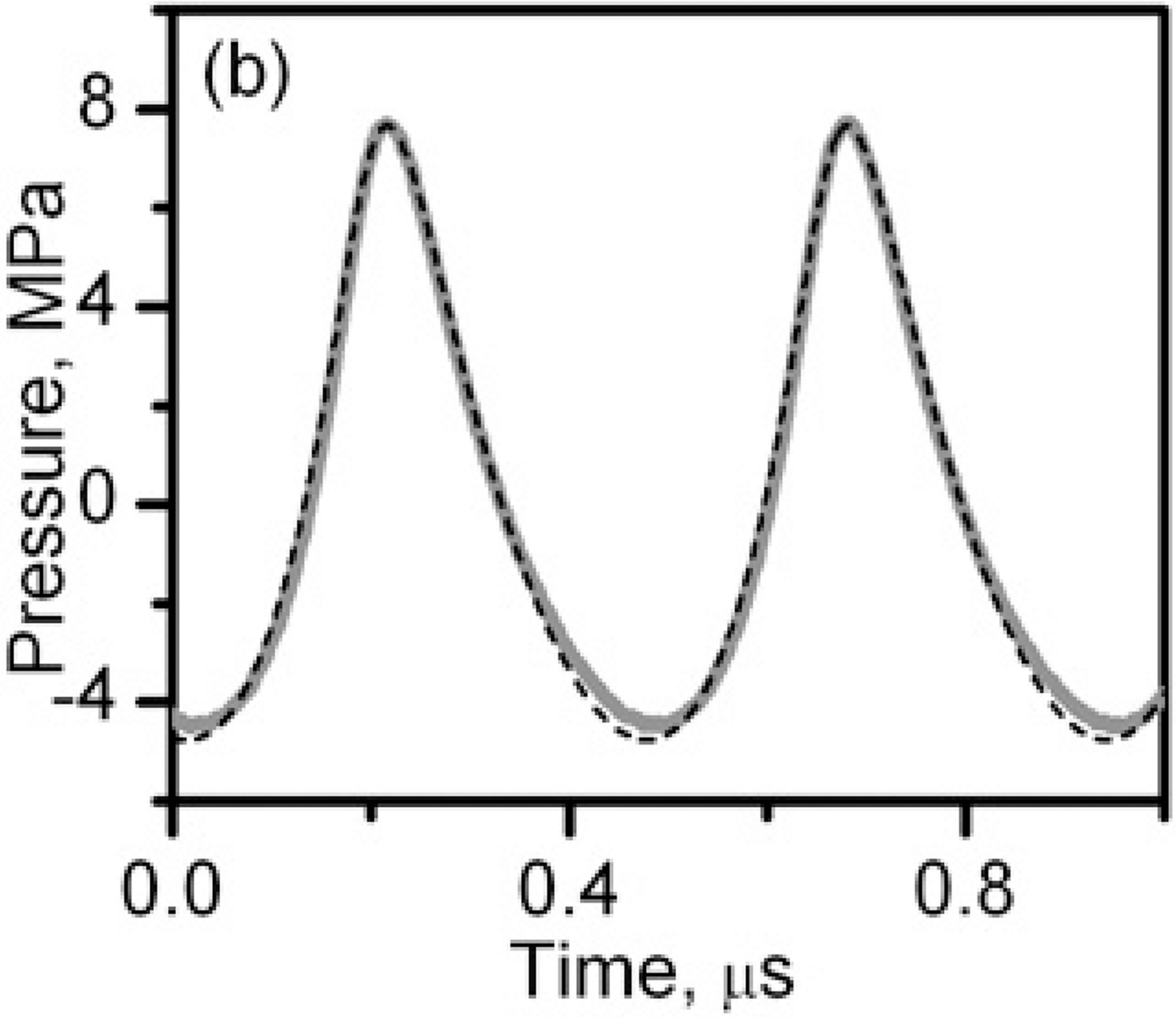

Figure 2.

In situ HIFU waveforms at the power output levels used to produce liquid, paste, and vacuolated thermal lesions **(a)** and solid thermal lesions **(b)**. The waveforms were measured by the FOPH behind a 12-mm thick layer of bovine heart tissue (thick grey curves) and modeled using the KZK equation and nonlinear derating approach (black dashed curves) (Khokhlova et al. 2011a).

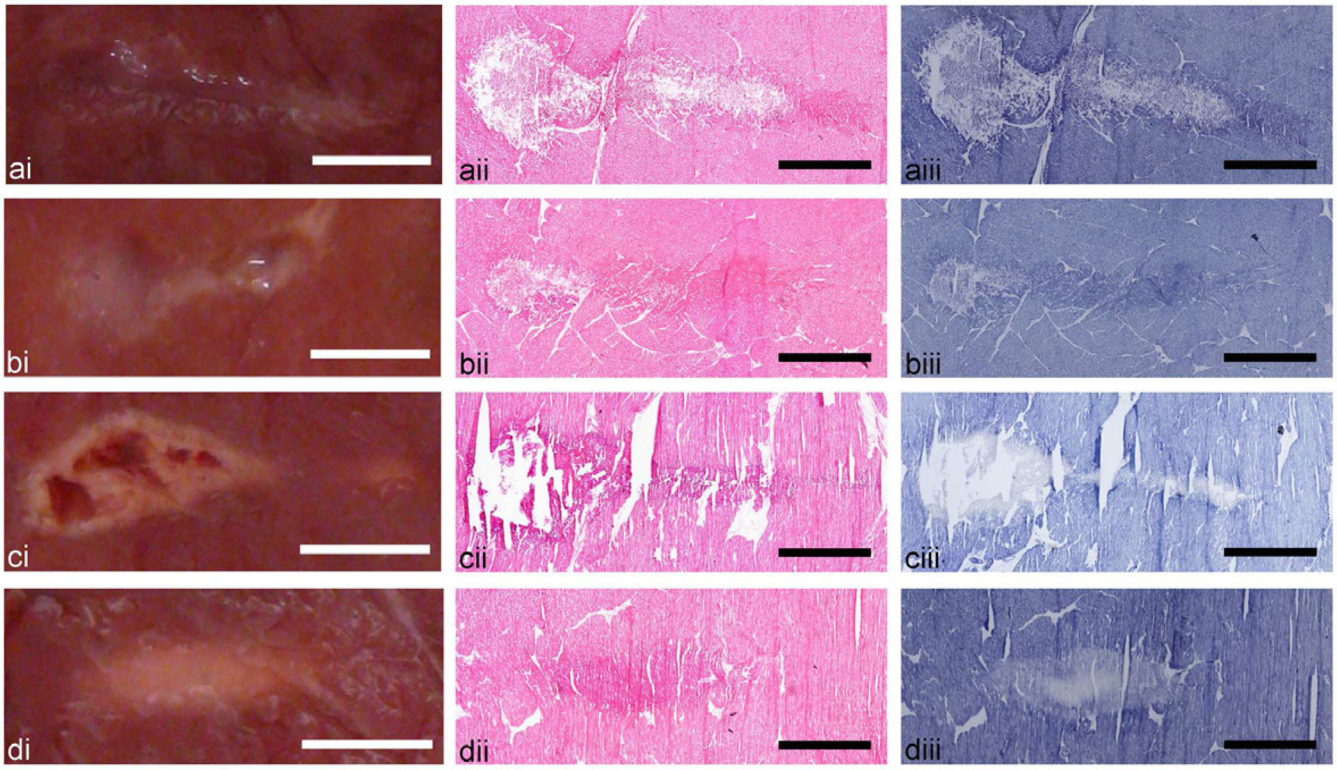

Figure 3.

Axial cross sections of the four types of HIFU lesions created in *ex vivo* bovine cardiac tissue: (a) liquid, (b) paste, (c) vacuolated thermal, and (d) solid thermal. Each lesion type is illustrated by (i) a representative photograph and histological images of consecutive frozen sections stained with (ii) H&E, revealing cellular structure, or (iii) NADH-d, revealing the extent of thermal damage. Lesions resulting from HIFU exposures that induce rapid boiling (a–c) are evident in both H&E and NADH stained sections as disrupted tissue. Thermal damage is indicated by the absence of dark blue NADH-d stain or by more eosinophilic (stained darker pink) areas in H&E stained sections (c, d) due to desiccation of cells. The NADH-d stained sections of neither liquid (a) nor paste (b) lesions show any indication of thermal damage. Scale bar represents 2 mm.

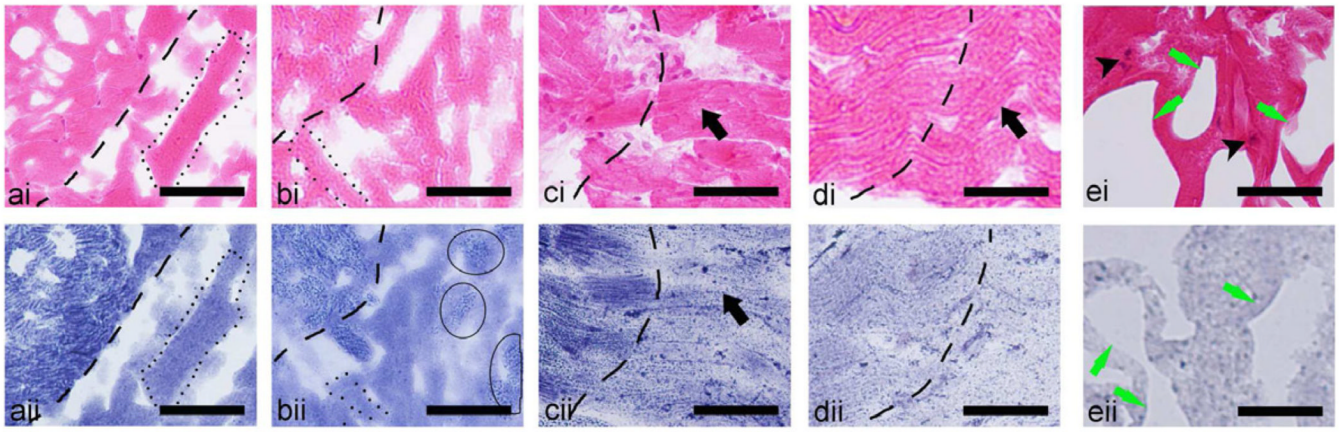

Figure 4.

Magnified histological images of consecutive frozen sections stained with (i) H&E (top row), or (ii) NADH-d (bottom row) of the four types of lesions induced by HIFU in *ex vivo* bovine cardiac muscle: (a) liquid, (b) paste, (c) the border of the vacuolated thermal, (d) solid thermal, and (e) the central part of the vacuolated thermal lesion. The dashed line in the images denotes the border between the intact tissue (to the left of the images) and the lesions (to the right of the images). (a) In the liquid lesion the border is very distinct in both H&E and NADH-d stained images. The complete liquefaction of tissue is evident from the absence of any native structure and formation of ice crystals (outlined by dotted lines). No nuclei (stained purple) are observed within the lesion contents in the H&E image and no thermal damage (unstained tissue) - in the NADH-d image. Similarly, the border of the paste lesion (b) is very distinct; however, t he lesion contains several fragments of un-liquefied tissue (outlined by the thin line). The tissue within the solid thermal (d) lesion appears as thermally fixed with minimal structural disruption (black arrows): very little difference from intact tissue is observed in the H&E (i) stained sections, whereas NADH-d (ii) stained sections demonstrate thermal damage. Note that the margins between fully thermally denatured and intact tissue is much broader than that for liquid and paste lesions, as shown by the gradual change in NADH stain hue at the border. Same was true for the very border of the vacuolated lesion (c), but in the bulk of the lesion large areas void of tissue were apparent (ei and eii, green arrows), and the nuclei were still present in some regions of the tissue (black arrowheads). Scale bar represents 50 μm.

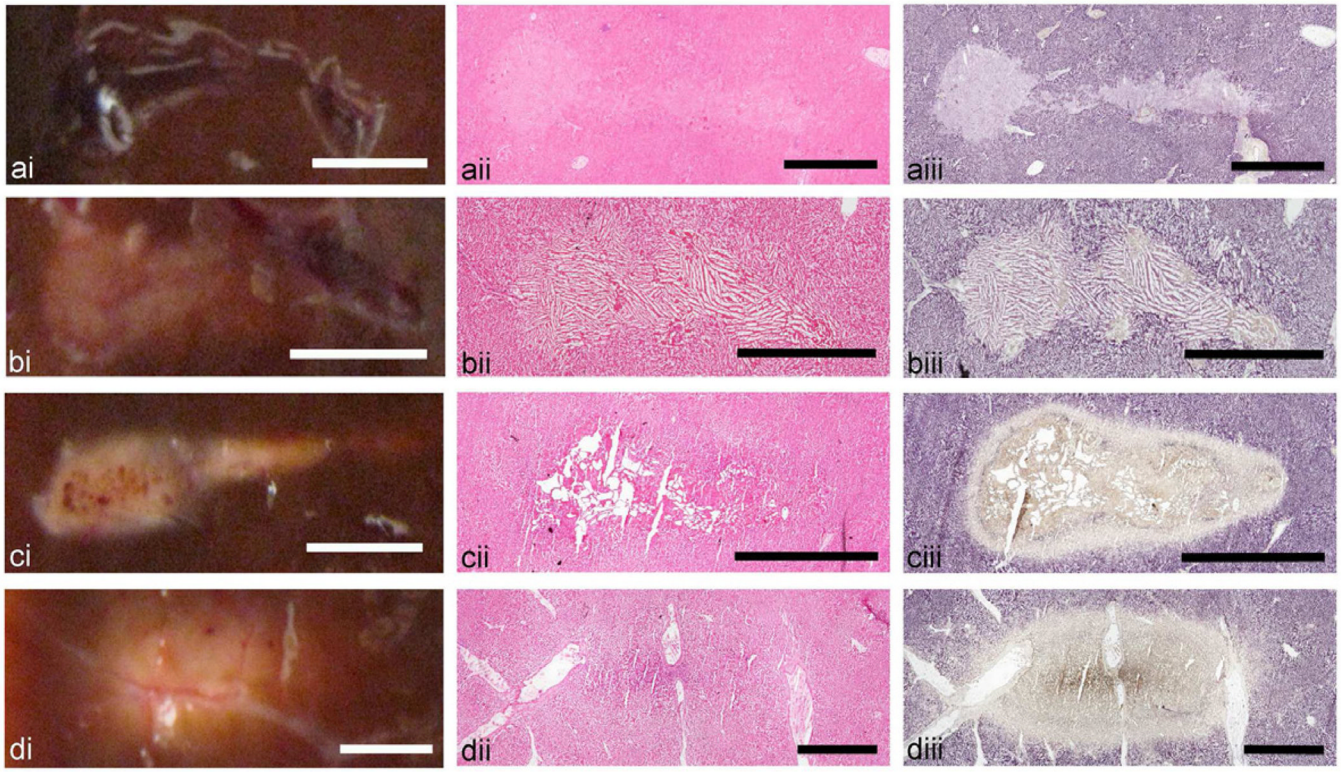

Figure 5.

Axial cross sections of the four types of HIFU lesions created in *ex vivo* bovine liver tissue: (a) liquid, (b) paste, (c) vacuolated thermal, and (d) solid thermal. Each lesion type is illustrated by (i) a representative photograph and histological images of consecutive frozen sections stained with (ii) H&E or (iii) NADH-d. Similarly to cardiac muscle (Fig. 3), gross visual observation provides mostly correct representation of the lesion contents. The liquid and paste lesions are clearly demarcated in both H&E and NADH stained sections as tissue lacking cellular structure (a,b). Thermal damage is present in some areas of the paste lesion (b), but absent in the liquid lesion (a). Both vacuolated thermal (c) and solid thermal (d) lesions are visible as the area of thermal damage, characterized by the absence of NADH-d stain. The cores of both lesions have a brown tint which may be due to increased tissue dehydration compared to the lesion edges. The vacuolated thermal lesion contains large areas void of tissue (d), whereas the solid thermal lesion appears as thermally fixed tissue with nearly intact cellular structure (c). Scale bar represents 2 mm.

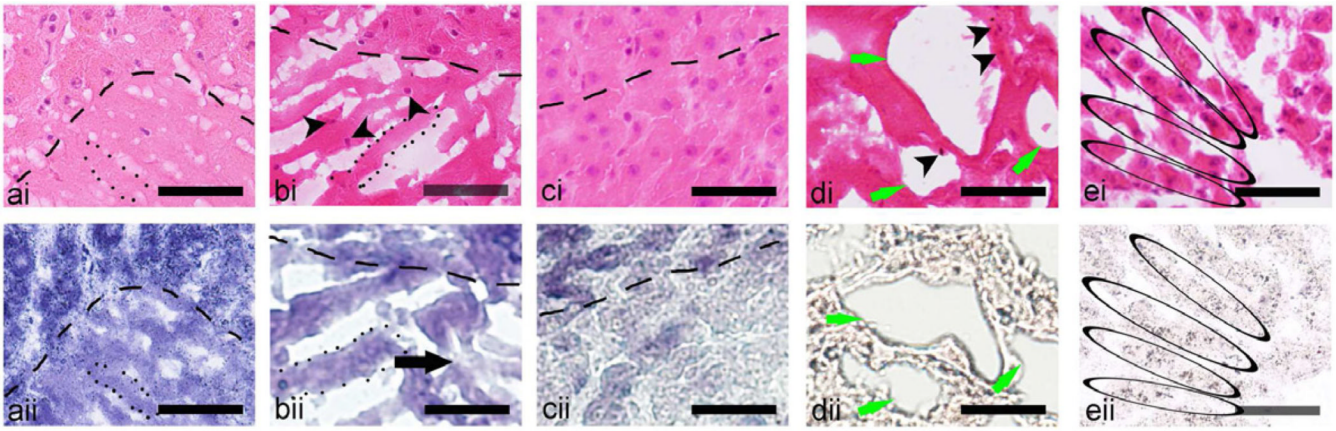

Figure 6.

Magnified histological images of consecutive frozen sections stained with (i) H&E or (ii) NADH-d of the four types of lesions induced by HIFU in *ex vivo* bovine liver: (a) liquid, (b) paste, (c) vacuolated thermal, and (d) solid thermal. The margins of the lesions (bottom of images) are outlined by a dashed line. In the liquid lesion (a), the margin is very distinct, a s the lesion contents were completely liquefied without any native structure present, as observed in the H&E stained section. There were almost no nuclei observed within the lesion contents and there was a lack of unstained tissue (thermally damaged) in the NADH-d stained liquid lesion. The content of the paste lesion (b) was also mostly liquefied, but included some un-liquefied tissue fragments, as indicated by the presence of nuclei (black arrow heads). There were some areas of slight thermal damage within the lesion as indicated by unstained tissue in the NADH-d stained (bii) section (black arrow). The frozen tissue artifact was pronounced in both liquid and paste lesions; the ice crystals are outlined by a dotted line in (a) and (b). The tissue at the margins of the vacuolated (d) and solid (c) thermal lesions appeared as thermally fixed, with minimal structural and with obvious thermal damage. At the center of the vacuolated thermal lesion the cellular structure was mostly disrupted, with large areas void of tissue (di and dii, green arrows), but several intact nuclei still observed (di, black arrow heads). At the center of the solid thermal lesion (e), the general liver structure was still present. The cords of hepatocytes were still prominent (black ovals) with cells remaining intact but with signs of coagulative necrosis: pyknosis, karyolysis, karyorrhexis and hyperchromasia. Scale bar represents 50 μm.

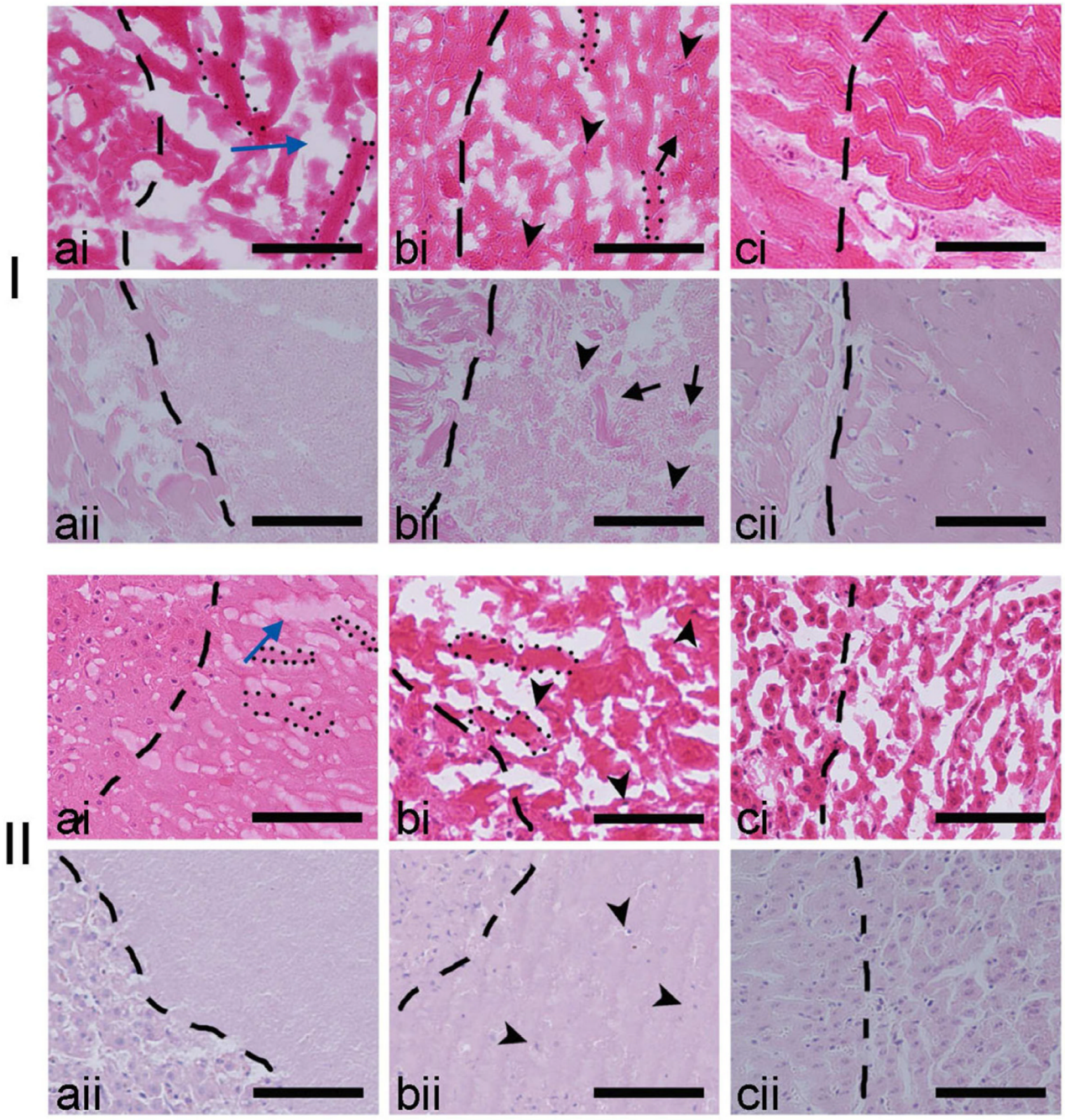

Figure 7.

Comparison of the H&E stained sections of fresh frozen (i) and formalin fixed (ii) lesions induced in bovine cardiac (I) and liver (II) tissue. The border of the lesions (to the right of images) is shown as the dashed line. Within the fresh frozen liquid (a) and paste (b) lesions in both tissues ice crystal formation was evident and resulted in voids (blue arrow) known as the freezing artifact, that is absent in the formalin fixed tissue. Within the paste lesion the intact nuclei (black arrow heads) and un-liquefied tissue fragments (black arrows) are better visualized in the formalin fixed sample (bii), although are discernible in the fresh frozen sample as well (bi). Fresh frozen and formalin fixed solid thermal lesions (c) are shown for comparison. Scale bar represents 100 μm.

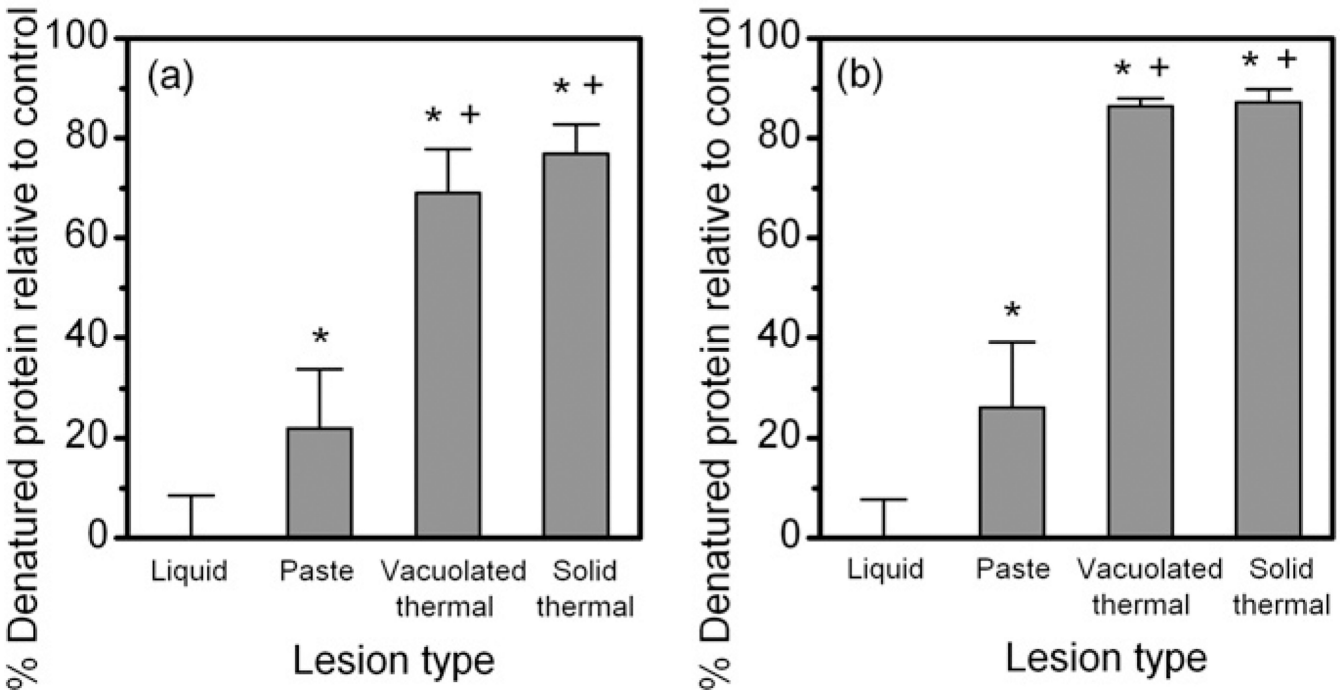

Figure 8.

Percent of denatured salt soluble protein extracted from the four lesion types (liquid, paste, solid, and vacuolated thermal) produced in bovine cardiac muscle (a) and bovine liver (b) relatively to control samples (n = 3–6). Pieces of tissue emulsified in a conventional blender were used as controls. "*" denotes significant difference from liquid lesion at the significance level of $p < 0.01$. "+" denotes significant difference from the paste lesion at the significance level of $p < 0.01$. Percent of soluble protein was used as a quantitative measure of the thermal effect since the solubility is lost with thermal denaturation.

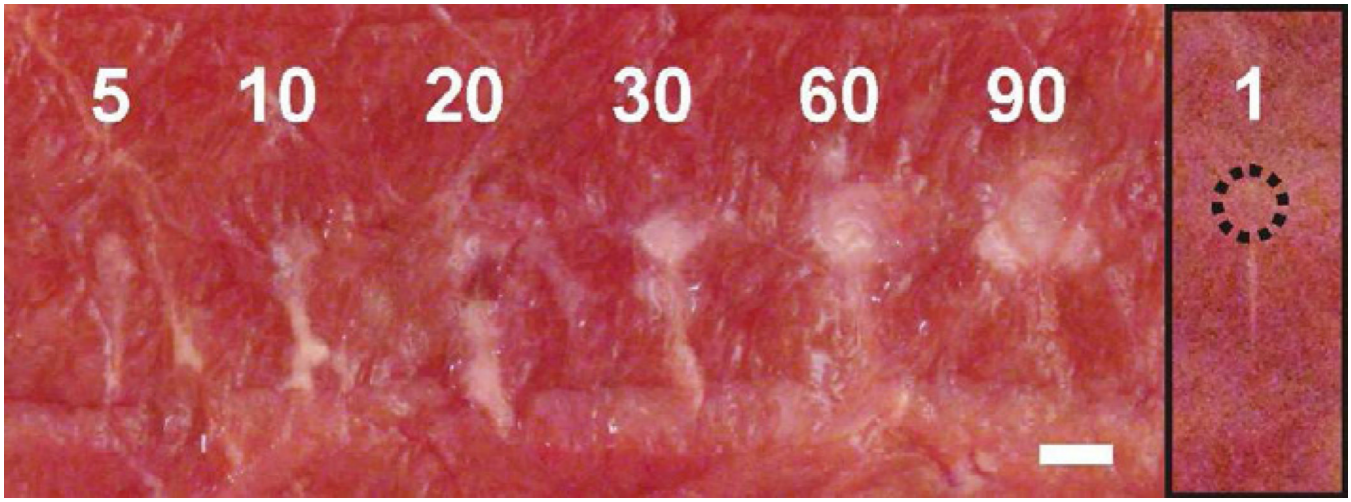

Figure 9.

A series of lesions induced in *ex vivo* bovine cardiac muscle using an increasing (5 – 90) number of 10-millisecond HIFU pulses delivered at a 1 Hz pulse repetition frequency. The corresponding *in situ* HIFU waveform is shown in Fig.1a. The number of pulses did not change the the type (“paste”) and the shape (“tadpole”) of the lesions. However, it affected their maximum width and length. Both of the lesion dimensions increased noticeably with the number of pulses up to 30, then reached saturation and virtually did not change starting from 60 pulses. The inset on the right shows the lesion resulting from a single pulse. The small circular void (outlined by a dotted line) at the anterior side of the upper lesion demonstrates, that even a single HIFU pulse, that induces millisecond boiling, can produce tissue emulsification. The scale bar is 2 mm.

Table 1

Summary of the pulsing protocol parameters – duty factor (*DF)* and pulse duration (τ) used to produce different types of HIFU lesions in bovine liver and cardiac tissues. The *in situ* HIFU peak intensity and the total HIFU-on time were the same for all the boiling histotripsy lesions – liquid, paste, and vacuolated thermal: 20 kW/cm^2 and 0.5 s, respectively. To produce a solid thermal lesion, a lower *in situ* intensity of 1.7 kW/cm^2 and continuous 20 s exposure was used. Two different regimes were employed to produce paste lesions in cardiac tissue for (a) histological evaluation and (b) protein analysis of the lesion contents.

Liquid	**Paste**		**Vacuolated thermal**	**Solid thermal**
	Liver	**Cardiac muscle**		
DF = 0.005, τ = 5 ms	*DF* = 0.01, τ = 20 ms	*(a) DF* = 0.01, τ = 10 ms	CW, τ = 500 ms	CW, τ = 20 s
		(b) DF = 0.01, τ = 20 ms		